

# Reductive Functionalization of Single-Walled Carbon Nanotubes with Lithium Metal Catalyzed by Electron Carrier Additives

Ainara García-Gallastegui,<sup>\*,†</sup> Isabel Obieta,<sup>†</sup> Izaskun Bustero,<sup>†</sup> Gorka Imbuluzqueta,<sup>†</sup> Jordi Arbiol,<sup>‡</sup> José Ignacio Miranda,<sup>§</sup> and Jesus M. Aizpurua<sup>\*,§</sup>

INASMET-Tecnalia, Paseo Mikeletegi 2, 20009 San Sebastian, Spain, TEM-MAT, Serveis Científicotecnics and EME/CeRMAE/IN<sup>2</sup>UB, Universitat de Barcelona, c/Lluís Soléi Sabaris, 1-3, 08028 Barcelona, CAT, Spain, and Joxe Mari Korta R&D Center, Departamento de Química Orgánica I, Universidad del País Vasco, Avda. Tolosa-72, 20018 San Sebastian, Spain

Received March 4, 2008. Revised Manuscript Received May 7, 2008

Lithium metal can be used to reduce single-walled carbon nanotubes (SWNT) to carbide-like species under the catalytic effect of di-*tert*-butyl-biphenyl (DTBP). The resulting nanotube polycarbanions show a significantly increased dispersability in THF and react “in situ” with trimethylchlorosilane, methyl methacrylate, and methyl *N*-acetamidoacrylate to afford covalently functionalized silyl nanotubes and polymer-wrapped SWNT. The density and average length of the polymer chains attached to the nanotube wall can be widely modified by varying the amount of monomer, lithium, and catalyst.

## Introduction

Since the discovery of multiwalled carbon nanotubes (MWNT) in 1991<sup>1</sup> and single-walled carbon nanotubes (SWNT) in 1993,<sup>2</sup> the carbon nanotubes (CNT) have become of great interest, both from a fundamental point of view and for their potential applications. Extraordinary mechanical and unique electronic properties<sup>3</sup> make them attractive candidates in diverse applications. However, further development is complicated by their difficult handling and, more particularly, by their tendency to form bundles in any solvents. Therefore, chemically modified CNT are necessary for their incorporation to inorganic, organic, or biological systems and, for this reason, research on superficial modification of CNT is growing at a rapid pace.<sup>4</sup>

CNT can be reduced to electron-enriched carbide-like species taking advantage of their “electron sink” properties. According to ab initio theoretical calculations,<sup>5</sup> transformation of CNT into carbanionic derivatives would be energetically more favored than related conversions into CNT free

radicals or carbocations. Likewise, carbanionic CNT are suitable intermediates to react with a variety of electrophilic reagents, providing a convenient synthetic entry to CNT with modified or functionalized sidewalls. For instance, Birch reduction with lithium or sodium “electron solvates”  $M^+[e^-(NR_3)_n]$  in ethylenediamine<sup>6</sup> or liquid ammonia containing methanol<sup>7</sup> has been used to hydrogenate SWNT. In combination with alkyl or aryl halides, this method affords the corresponding alkyl- or aryl-substituted SWNT through a putative reductive alkylation reaction pathway,<sup>8</sup> whereas addition of acrylic ester monomers promotes anionic polymerization onto the SWNT wall.<sup>9</sup> On the other hand, alkyl carbanions (e.g., *sec*-butyl lithium) also add to SWNT<sup>10</sup> to generate anionic sites suitable for “grafting from” anionic polymerization of *tert*-butyl acrylate (*t*-BA) and block copolymerization of *t*-BA and methyl methacrylate (MMA).<sup>11</sup> Finally, lithium and sodium naphthalenide radical

\* To whom correspondence should be addressed. E-mail: jesumaria.aizpurua@ehu.es.

<sup>†</sup> INASMET-Tecnalia.

<sup>‡</sup> Universitat de Barcelona.

<sup>§</sup> Universidad del País Vasco.

(1) Iijima, S. *Nature* **1991**, *354*, 56–58.

(2) (a) Iijima, S.; Ichihashi, T. *Nature* **1993**, *363*, 603–605. (b) Bethune, D. S.; Kiang, C. H.; de Vries, M. S.; Gorman, G.; Savoy, R.; Vazquez, J.; Bayers, R. *Nature* **1993**, *363*, 605. (c) Endo, M.; Takeuchi, K.; Igarashi, S.; Kobori, K.; Shiraishi, M.; Kroto, H. W. *Phys. Chem. Solids* **1993**, *54*, 1841.

(3) (a) Dresselhaus, M. S.; Dresselhaus, G.; Eklund, P. C. *Science of Fullerenes and Carbon Nanotubes*; Academic Press: San Diego, CA, 1996; Vol. 1. (b) Saito, R.; Dresselhaus, M. S.; Dresselhaus, G. *Physical Properties of Carbon Nanotubes*; Imperial College Press: London, 1998.

(4) (a) Bahr, J. L.; Tour, J. M. *J. Mater. Chem.* **2002**, *12*, 1952–1958. (b) Tasis, D.; Tagmatarchis, N.; Georgakilas, V.; Prato, M. *Chem. Eur. J.* **2003**, *9*, 4000–4008. (c) Tasis, D.; Tagmatarchis, N.; Bianco, A.; Prato, M. *Chem. Rev.* **2006**, *106*, 1105–1136.

(5) Mylvaganam, K.; Zhang, L. C. *J. Phys. Chem. B* **2004**, *108*, 15009–15012.

(6) Chen, Y.; Haddon, R. C.; Fang, S.; Rao, A. M.; Eklund, P. C.; Lee, W. H.; Dickey, E. C.; Grulke, E. A.; Pendergrass, J. C.; Chavan, A.; Haley, B. E.; Smalley, R. E. *J. Mater. Res.* **1998**, *13*, 2423–2431.

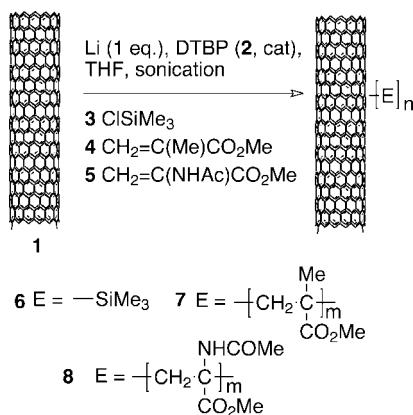
(7) Pekker, S.; Salvetat, J.-P.; Jakab, E.; Bonard, J.-M.; Forró, L. *J. Phys. Chem. B* **2001**, *105*, 7938–7943.

(8) (a) Liang, F.; Sadana, A. K.; Peera, A.; Chattopadhyay, J.; Gu, Z.; Hauge, R. H.; Billups, W. E. *Nano Lett.* **2004**, *4*, 1257–1260. (b) Borondics, F.; Bokor, M.; Matus, P.; Tompa, K.; Pekker, S.; Jakab, E. *Fullerenes, Nanotubes, Carbon Nanostruct.* **2005**, *13*, 375–382. (c) Chattopadhyay, J.; Sadana, A. K.; Liang, F.; Beach, J. M.; Xiao, Y. X.; Hauge, R. H.; Billups, W. E. *Org. Lett.* **2005**, *7*, 4067–4069. (d) Borondics, F.; Jakab, E.; Pekker, S. *J. Nanosci. Nanotechnol.* **2007**, *7*, 1551–1559.

(9) Liang, F.; Beach, J. M.; Kobashi, K.; Sadana, A. K.; Vega-Cantu, Y. I.; Tour, J. M.; Billups, W. E. *Chem. Mater.* **2006**, *18*, 4764–4767.

(10) (a) Viswanathan, G.; Chakrapani, N.; Yang, H.; Wei, B.; Chung, H.; Cho, K.; Ryu, Ch. Y.; Ajayan, P. M. *J. Am. Chem. Soc.* **2003**, *125*, 9258–9259. (b) Blake, R.; Gun'ko, Y. K.; Coleman, J.; Cadek, M.; Fonseca, A.; Nagy, J. B.; Blau, W. J. *J. Am. Chem. Soc.* **2004**, *126*, 10226–10227. (c) Chen, S.; Shen, W.; Wu, G.; Chen, D.; Jiang, M. *Chem. Phys. Lett.* **2005**, *402*, 312–317.

(11) Chen, S.; Chen, D.; Wu, G. *Macromol. Rapid Commun.* **2006**, *27*, 882–887.

**Scheme 1. Lithium-Promoted “One-Pot” Functionalization of SWNT Catalyzed by 4,4'-Di-*tert*-butyl-biphenyl (DTBP, 2)**


anions have also been shown to generate carbanionic SWNT, which can be subsequently alkylated with alkyl halides.<sup>12</sup>

Direct reduction of CNT with metals remains a reluctant process. In contrast to fullerene counterparts, which are reduced directly to the corresponding fullerenes with lithium metal upon vigorous sonication,<sup>13</sup> CNT are doped with alkali metals only under harsh conditions.<sup>14</sup> Herein we report a chemical method to prepare carbanionic SWNT under experimentally mild conditions using lithium metal as electron source and catalytic amounts of 4,4'-di-*tert*-butyl-biphenyl (DTBP) as electron carrier. Incorporation of electrophiles to the reduction reaction and, more particularly of acrylic ester monomers, permits the preparation of covalently modified SWNT–poly(acrylate) materials in a “one-pot” transformation starting from pristine nanotubes.

### Experimental Section

**Materials and Equipment.** SWNT soot was purchased from Nanocyl (Nanocyl-1100) and was used without further purification. Filtrations were performed on nylon HNMP 47 mm/0.45 μm and fluoropore FGLP 47 mm/0.22 μm membranes from Millipore. Granular lithium (99%), DTBP, trimethylchlorosilane, and methyl *N*-acetamidoacrylate were used as purchased from Sigma-Aldrich. THF was distilled over sodium wire and benzophenone prior to use. MMA was used after stabilizer removal by washing successively with 1 M NaOH, saturated NaHCO<sub>3</sub>, and water, drying over MgSO<sub>4</sub>, and deoxygenation by argon bubbling. All manipulations were conducted under argon in an inert gas box InerTec glovebox type ITA 14, incorporating a vacuum transfer chamber.

**General Procedure for SWNT Functionalization.** (Scheme 1; 1 → 6–8) In a flame-dried round-bottomed 25 mL flask, SWNT (12 mg), granular lithium (7 mg, 1 mmol), and DTBP additive (26 mg, 0.1 mmol) were introduced under argon. THF (10 mL) was injected via syringe, and the mixture was sonicated during 1 h at room temperature. The corresponding electrophile (3–5; see Tables 1 and 2 for details) (0.03–10 mmol) was added via syringe, and the mixture was sonicated until total dissolution of lithium. After solvent evaporation in vacuo, electrophile excess and polymers

**Table 1. Effect of Electron Carrier Additives on the Reductive Trimethylsilylation of SWNT with Lithium and Trimethylchlorosilane 3**

entry no. <sup>a</sup>	SWNT (1) (mmol)	lithium (mmol)	additive (mmol)	ClSiMe <sub>3</sub> (3) (mmol)	time (h) <sup>b</sup>	Si/C in (6) mol %
1	1	1	naphthalene (0.1)	10	7	1.2
2	1	1	naphthalene (6)	10	1.5	0.7
3	1	1	DTBP (0.1)	10	7	2.0
4	1	5	(Me <sub>2</sub> N) <sub>3</sub> P=O (6)	10	1.5	1.0
5(C1)	1	5		10	7	>0.1

<sup>a</sup> All reactions were performed in THF according to the General Procedure for SWNT Functionalization section. <sup>b</sup> Required for complete dissolution of lithium.

**Table 2. “Grafting from” Anionic Polymerization of SWNT with Methyl Methacrylate Promoted by Lithium and Catalyzed by DTBP**

entry no. <sup>a</sup>	SWNT (1) (mmol)	lithium (mmol)	DTBP (2) (mmol)	MMA (4) (mmol)	time (h) <sup>b</sup>	wrapping diameter (nm) <sup>c</sup>
1	1	1	0.1	10.0	1.5	120–130
2	1	1	0.1	1.5	7	100–110
3	1	1	0.1	0.1	8	70–80
4	1	1	0.1	0.03	8	30–40
5	1	0.5	0.05	10.0	1.5	50–60
6(C2)	1	1		10	1.5 <sup>d</sup>	
7(C3)	1	1	0.1	10	1	

<sup>a</sup> All reactions were performed in THF and worked up according to the General Procedure for SWNT Functionalization section. <sup>b</sup> Required for complete dissolution of lithium. <sup>c</sup> Average values of polymer wrapping determined by SEM. Pristine SWNT average diameter = 10 nm. <sup>d</sup> Nearly all lithium remained unchanged after reaction.

nonbonded to SWNT were removed by washing with toluene or dichloromethane, followed either by filtration in vacuo, by centrifugation, or by extraction, depending on the electrophile used. SWNT-derived products (6–8) were extensively washed with dichloromethane (DCM) and diethylether (Et<sub>2</sub>O), and after filtration through a fluoropore membrane, they were dried overnight under argon at 105 °C.

**Characterization.** FTIR spectra were recorded on a Nicolet Magna-IR 750 spectrometer equipped with a monochromatic IR-ray source (Ever-Glo mid-IR) and a DTGS-KBr detector, using dried KBr-embedded pellets. NMR heteronuclear multiple-quantum correlation (HMQC) <sup>1</sup>H/<sup>13</sup>C experiments were performed at 300 K in CDCl<sub>3</sub> using a Bruker-AVANCE-500 spectrometer, and δ values (ppm) are reported as relative to residual chloroform (δH, 7.26 ppm; δC, 77.16 ppm). Thermogravimetric measurements were carried out on a TGA-Q500 TA Instruments equipment under nitrogen flow at a scan rate of 10 °C/min from 100 to 1000 °C and keeping the temperature at 100 °C and at 1000 °C for 20 min. Quantitative analysis was determined using an energy-dispersive X-ray (EDX) diffractometer, Oxford model INCA-300, coupled to a scanning electron microscope (SEM) JEOL JSM-5910 LV, setting the acceleration voltage at 20 kV. SEM observations were also conducted using a JEOL JSM-7000F field emission source. High-resolution transmission electron microscope (HRTEM) micrographs were obtained using a JEOL 2010F field emission gun microscope, working at 200 kV with a point-to-point resolution of 0.19 nm.

### Results and Discussion

**Electron-Transfer Additive Screening.** Among the many organic molecules known to accept electrons from alkali metals, we focused our attention on several anion radical promoters.<sup>15</sup> In particular, naphthalene<sup>12</sup> and DTBP, an extremely efficient electron carrier developed by Yus.<sup>16</sup> We also became interested in hexamethylphosphoric triamide

- (12) (a) Petit, P.; Mathis, C.; Journet, C.; Bernier, P. *Chem. Phys., Lett.* **1999**, *305*, 370–374. (b) Penicaud, A.; Poulin, P.; Derre, A.; Anglaret, E.; Petit, P. *Fullerenes, Nanotubes, Carbon Nanostruct.* **2005**, *127*, 8. (c) Penicaud, A.; Poulin, P.; Derre, A.; Anglaret, E.; Petit, P. *J. Am. Chem. Soc.* **2005**, *127*, 8–9, and references therein (ref 7d)
- (13) Bausch, J. W.; Prakash, K. S.; Olah, G. A.; Tse, D. S.; Lorents, D. C.; Bae, Y. K.; Malhotra, R. *J. Am. Chem. Soc.* **1991**, *113*, 3205–3206.
- (14) Duclaux, L. *Carbon* **2002**, 1751–1764.

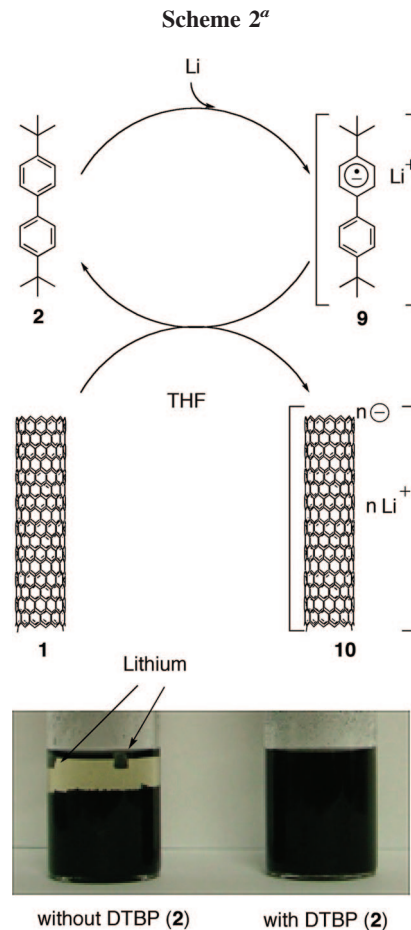
(HMPA), owing to its combined ability to partially debundle pristine SWNT ropes<sup>17</sup> and to form anion radicals<sup>18</sup> with lithium.

Preliminary experiments were carried out to check the solubilizing effect of lithium on SWNT by sonicating THF suspensions of the nanotubes and metal rods in the presence of catalytic amounts (typically 10 mol %) of naphthalene, DTBP, and HMPA. All instances compared favorably with a control experiment conducted without additives and solubilization of lithium metal and permanent dispersion of SWNT (several weeks) was observed, albeit overstoichiometric amounts were required in the case of HMPA. Naphthalene and HMPA gave strongly colored solutions of deep green and purple color, respectively, whereas DTBP gave uncolored solutions. These results were rationalized in terms of the electron-transfer catalytic cycle shown in Scheme 2. The highly reactive and sterically hindered DTBP arene anion radical **9** was thought to enable a sequential electron transfer on the SWNT surface to form the carbanionic SWNT species **10**, which was separated from the bundles and stayed in solution due to the mutual electrostatic repulsion between individual tubes, as confirmed by long-term solution homogeneity.

In order to compare the relative efficiency of the catalysts checked below and to set the basis for the development of a “one-pot” procedure for the trapping of carbanionic SWNT **10** by electrophiles, we conducted the experiments collected in Table 1. Silylation with trimethylchlorosilane **3** was chosen as a test reaction (Scheme 1, transformation **1** → **6**), and EDX analysis was used to quantify the Si/C molar percentage in each product sample. In all cases, modest but clearly appreciable incorporation of silicon to the SWNT derivative **6** was observed, showing that DTBP additive (entry 3) provided the highest Si/C ratio under similar reaction conditions. These functionalization densities were comparable to those (0.4–6.4 mol %) reported by Borondics et al. for related Birch-type alkylation reactions.<sup>8d</sup> Surprisingly, increasing amounts of carrier additive did not lead to higher silicon incorporation (compare entries 1 and 2). Finally, a control experiment (C1, entry 5), conducted in the absence of DTBP additive, led to the recovery of unchanged SWNT.

Silylated product **6** gave stable dispersions in hexane and was characterized by FTIR analysis (see Figure 1). The Si–(CH<sub>3</sub>)<sub>3</sub> moiety attached to the SWNT displayed characteristic bands at 1251 cm<sup>-1</sup>, assigned to the symmetric deformation vibration of methyl groups, and at 874 cm<sup>-1</sup>, corresponding to the Si–CH<sub>3</sub> bond oscillation. The weak intensity of these signals was in good agreement with the low level of silicon incorporation measured by EDX. These preliminary studies indirectly supported the formation of carbanionic SWNT **10** as a reaction intermediate and

- (15) Recently, the one-electron reaction of benzophenone radical anion with SWNT has been described: Wei, L.; Zhang, Y. *Eur. Chem. Phys. Lett.* **2007**, 142–144.
- (16) Ramón, D. J.; Yus, M. *Eur. J. Org. Chem.* **2000**, 225–237.
- (17) Ausman, K. D.; Piner, R.; Lourie, O.; Ruoff, R. S.; Korobov, M. J. *Phys. Chem. B* **2000**, *104*, 8911–8915.
- (18) (a) Normant, H.; Cuvigny, T.; Normant, J.; Angelo, B. *Bull. Soc. Chim. Fr.* **1965**, 3441–3446. (b) Picard, J. P.; Grelier, S.; Constantieux, T.; Dunogues, J.; Aizpurua, J. M.; Palomo, C.; Petraud, M.; Barbe, B.; Lunazzi, L.; Leger, J. M. *Organometallics* **1993**, *12*, 1378–1385.



<sup>a</sup> Top: lithium-mediated formation of “carbanionic SWNT” (**10**) promoted by DTBP anion radical, **9**. Bottom: reaction mixtures of SWNT and lithium in THF after 7 h of sonication (left) in the absence of DTBP and (right) in the presence of 10 mol % DTBP. Pictures were taken 1 h after reaction completion.

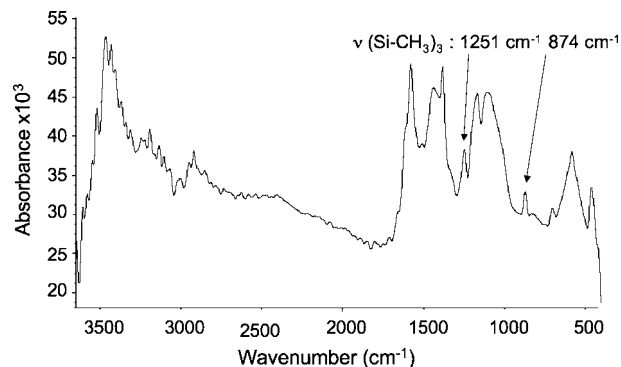


**Figure 1.** FTIR spectrum of trimethylsilylated SWNT **6**, prepared according to entry 3 in Table 1.

confirmed DTBP arene as the catalyst of choice to promote electron transfer from lithium to SWNT in further reactions.

**Anionic Polymerization of Methyl Methacrylate from Carbanionic SWNT.** Anionic polymerization of MMA onto carbanionic SWNT is known to occur under Birch reduction conditions in liquid ammonia, but the protic character of the medium causes partial reduction of the nanotube wall<sup>8c</sup> and limits the polymerization degree to a short range. For instance, Liang et al. have reported wrapping diameters of only 2.6 nm for HiPCO-SWNT of 0.6–1.3 nm



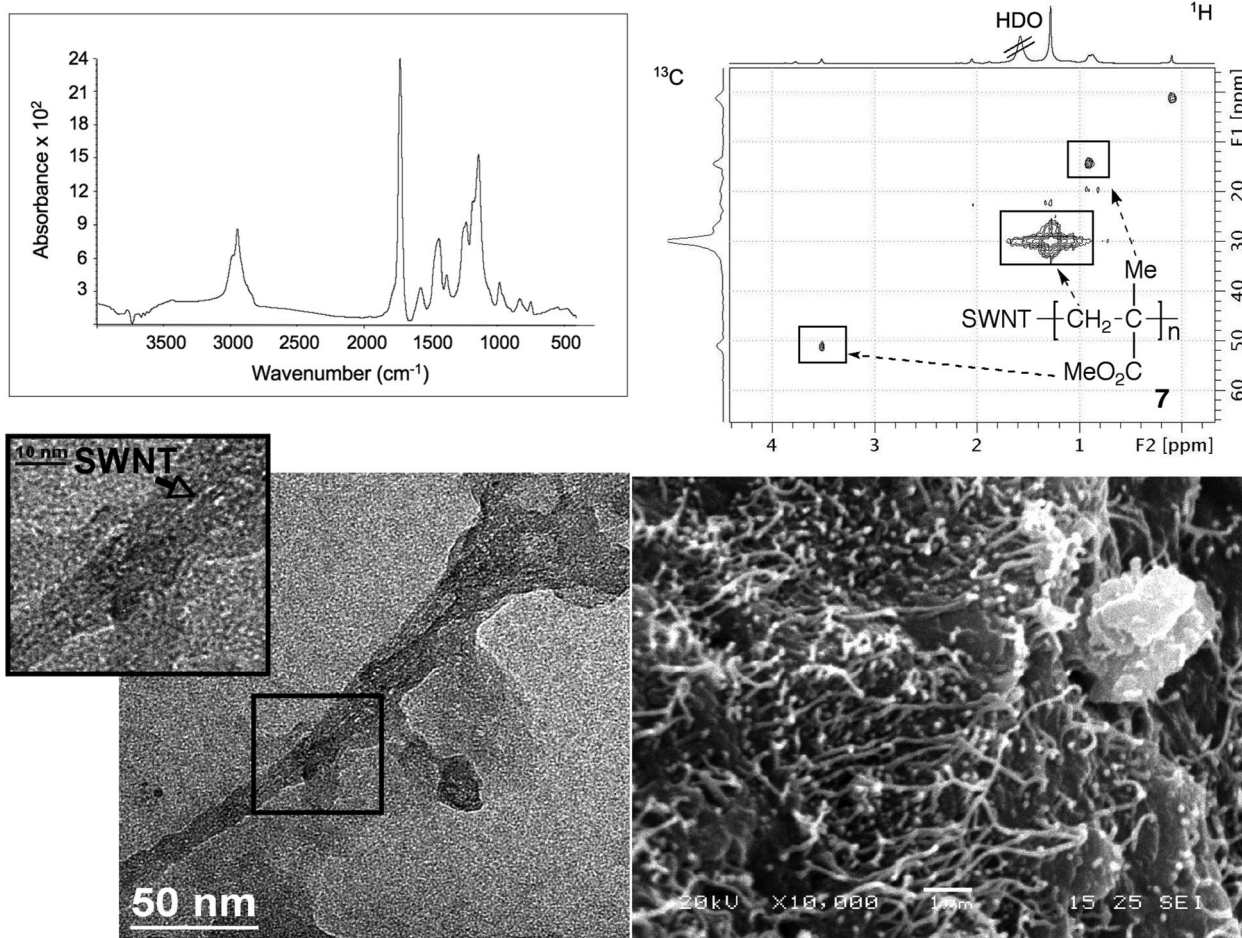


**Figure 2.** Chemical and morphological characterization of SWNT–poly(methyl methacrylate) **7**, prepared according to entry 1 in Table 2. Top: FTIR spectrum (left);  $^1\text{H}/^{13}\text{C}$  HMQC NMR spectrum (right). Bottom: HRTEM image, scale bar 50 nm, and 10 nm in magnification (left); SEM image, magnification 10 000 $\times$ , scale bar 1  $\mu\text{m}$  (right).

average diameter.<sup>9</sup> It is also known that MMA fails to polymerize from alkyl-SWNT carbanions created by *sec*-BuLi addition in THF.<sup>11</sup>

With the aim to explore the potential of the catalytically generated carbanionic SWNT **10** as an anionic polymerization initiator of MMA **4** in THF, we studied the formation of poly(methyl methacrylate) (PMMA)-wrapped SWNT material **7** (Scheme 1) under variable concentrations of monomer, lithium, and catalyst (Table 2). We found that in all instances (entries 1–5) different SWNT–PMMA materials **7** were formed and, more interestingly, that their wrapping diameter could be modified within a wide range, comprising average values from 30 to 130 nm for Nanocyl-SWNT of 10 nm average diameter. Decreasing of the MMA/SWNT ratio resulted in a moderate thinning of the PMMA layer (compare entries 1–4), which was attributed to the formation of shorter grafted polymer chains. Likewise, a reduction of the amount of lithium or DTBP catalyst with respect to SWNT gave rise to a more dramatic PMMA layer thinning (compare entries 1 and 5), which was associated to the diminution of carbanionic polymerization sites onto the nanotube intermediate **10**. Finally, we conducted control experiments C2 and C3 (entries 6, 7), to confirm that DTBP catalyst is necessary to promote polymerization of MMA

onto SWNT and that lithium/DTBP system is able to initiate the polymerization of MMA in the absence of SWNT.

SWNT–PMMA derivative **7**, obtained according to the conditions of entry 1 in Table 2 and purified by repeated washing with a good PMMA solvent (toluene), was submitted to chemical and morphological characterization.<sup>19</sup> As shown in Figure 2, the FTIR spectrum displayed characteristic bands at 1740  $\text{cm}^{-1}$ , assigned to the ester carbonyl (C=O) group, and at 1050–1300  $\text{cm}^{-1}$  associated to the ester vibration bands. In addition, an NMR  $^1\text{H}/^{13}\text{C}$  correlation experiment (HMQC) clearly showed the cross peaks of the  $\alpha\text{Me}$  (0.95/15.0 ppm),  $\text{CH}_2$  (1.33/29.9 ppm) and  $\text{CO}_2\text{Me}$  (3.56/51.1 ppm) groups. The morphology shown by SEM microphotograph was consistent with a homogeneous wrapping of PMMA around the extensively debundled nanotubes. Finally, HRTEM micrographs provided confirmation of the high relative contents of polymer present in the grafted SWNT and were consistent with the polymer wrapping diameter measured by SEM. The modified SWNT observed

(19) Attempts to estimate the SWNT sidewall modification measuring the  $I_D/I_G$  ratio by Raman spectroscopy met with failure because of the fluorescence induced by the laser light at wavelengths of 514 nm (green) and 785 nm (red). For related behavior, see: (a) Sun, Y.; Wilson, S. R.; Schuster, D. I. *J. Am. Chem. Soc.* **2001**, *123*, 5348–5349. (b) Wunderlich, D.; Hauke, F.; Hirsch, A. *Chem. Eur. J.* **2008**, *14*, 1607–1614.

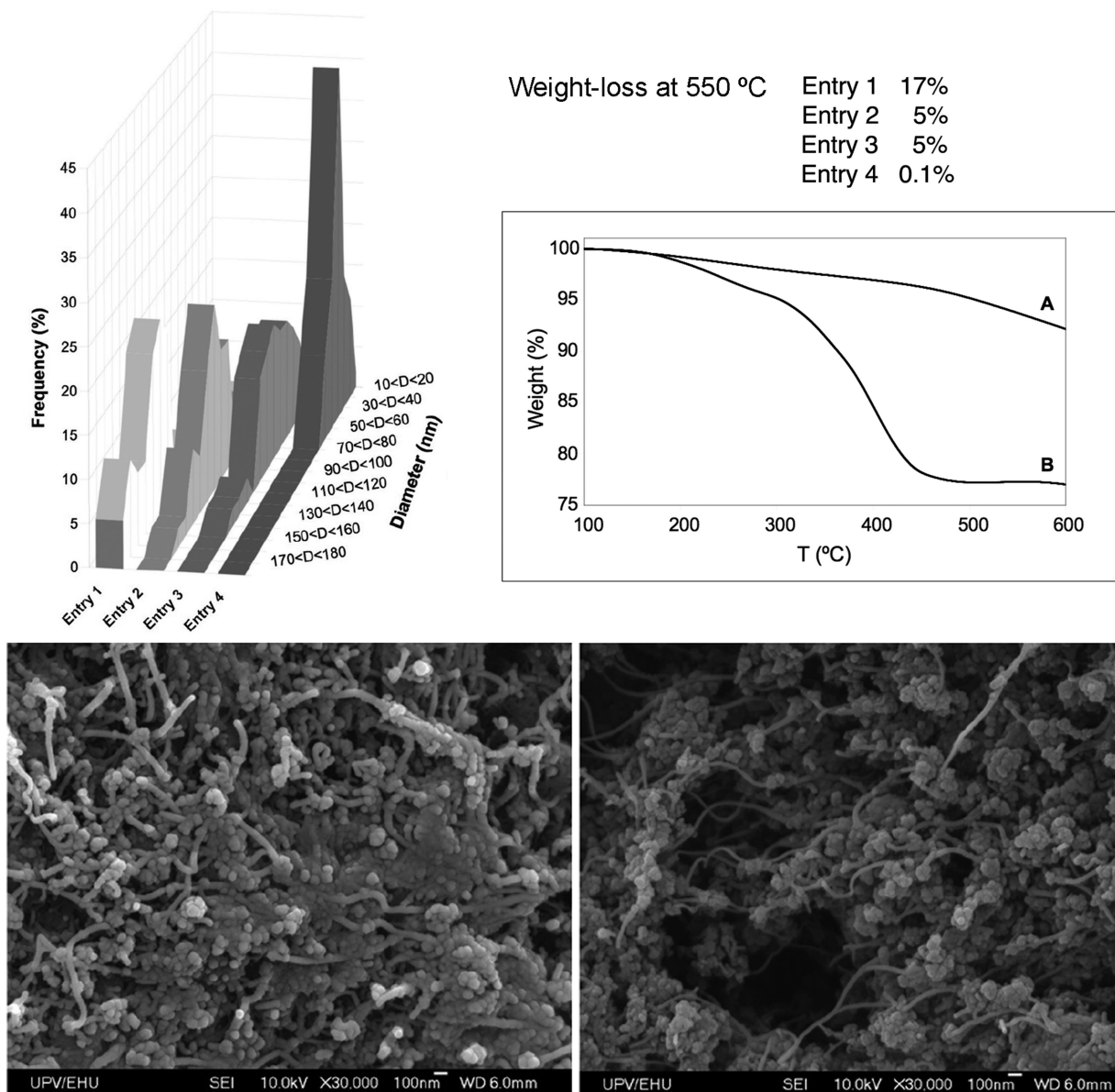


**Figure 3.** Morphological (SEM) and TGA characterization of SWNT–poly(methyl methacrylate) 7 samples prepared according to Table 2. Top: diameter distribution histograms for samples from entries 1–4 (left); TGA for samples from entries 1–4 and thermogram curves of (A) pristine SWNT and (B) sample from entry 1 (right). Bottom: comparison of SEM microphotographs for samples from entry 5 (left) and entry 6 (right). Magnification 30 000 $\times$ , scale bar 100 nm.

in the magnified HRTEM image clearly showed NT walls covered by a thick amorphous layer attributed to the PMMA.

Additional samples of SWNT–PMMA 7, obtained according to the reaction conditions disclosed in entries 1–4 in Table 2, were examined by SEM to determine their polymer wrapping diameter distribution. As outlined before, lowering the MMA monomer feed from 10 mmol (entry 1) to 0.03 mmol (entry 4) correlated satisfactorily with the average polymer wrapping diameter reduction observed for the corresponding products, which decreased from 120–130 nm (entry 1) to 30–40 nm (entry 4). Results collected in Figure 3 provided evidence of a variable diameter distribution, suggesting the existence of a considerable variation in the length of PMMA chains attached to the nanotube wall in each sample. This distribution was quite broad at high monomer feeds (entries 1–3) but became considerably

narrower at lower feeds (entry 4). Comparison of identically magnified SEM microphotographs of PMMA-grafted SWNT samples obtained according to entries 5 and 6 in Table 2 is also shown in Figure 3 (bottom) and puts into evidence the striking effect of the DTBP initiator amount on the thickness of the SWNT wall-wrapped polymer. Decreasing the relative amount of lithium and DTBP to a half, while keeping the MMA feed unchanged, resulted in a reduction of the average wrapping diameter from 120–130 nm (entry 1) to 50–60 nm (entry 5). Finally, total elimination of DTBP led to the recovery of unaltered SWNT (entry 6). The extent of the PMMA functionalization in SWNT products 7 from entries 1–4 was further studied by TGA of the degassed samples. Figure 3 (top right) shows the loss of weight of pristine SWNT compared to SWNT product 7 from entry 1, which displays a characteristic PMMA degradation slope at 450 °C. A weight



loss of 17% was calculated for the sample at 550 °C taking into account the relative degradation of the pristine SWNT (6%) at such temperature. Weight losses for products from entries 1–4 measured under identical conditions are also collected in the figure showing a decreasing percentage of final wrapped polymer when lower initial monomer quantities are used to feed the polymerization. These results confirm the preceding microscopy observations and strongly suggest that a much wider range of PMMA polymer chain lengths and grafting densities than those shown here can be obtained by making different combinations of MMA feed and lithium/DTBP ratios. They also demonstrate the suitability of catalytically generated carbanionic SWNT **10** as efficient sources for the anionic polymerization of acrylic monomers.

**Anionic Polymerization of  $\alpha,\beta$ -Dehydroamino Acid Esters from Carbanionic SWNT.** The  $\alpha$ -amino acid motif, occurring in peptides and protein biopolymers, has evident structural similarities with the  $\alpha$ -aminoacrylate ( $\alpha,\beta$ -dehydroamino acid ester) monomers. Although preparation of SWNT anchoring the poly( $\alpha$ -aminoacrylate) moiety might provide the access to nanotube materials with high biocompatibility, to the best of our knowledge no functionalization of SWNT with the readily available  $\alpha,\beta$ -dehydroamino acid esters<sup>20</sup> has been reported yet. Thus, under similar conditions to those used previously to grow MMA onto SWNT wall (Table 2, entry 1), methyl *N*-acetamidoacrylate **5** was reacted with “in situ” prepared carbanionic SWNT **10** to afford the expected SWNT–poly(methyl  $\alpha$ -acetamidoacrylate) **8** (Scheme 1). Functionalization of the nanotube wall was fully confirmed by FTIR analysis, and SEM images (Figure 4) clearly revealed a morphology consisting of nanotube structures uniformly covered with polymer material to an average wrapping diameter of about 70 nm.

### Conclusion

We have demonstrated that catalytic amounts of DTBP efficiently promote the formation of carbanionic SWNT in THF from pristine nanotubes and lithium. When the reduction reaction is carried out in the presence of MMA, different PMMA-grafted SWNT are obtained with a wide range of average wrapping diameters depending on the lithium/DTBP/MMA/SWNT proportions used for the functionalization

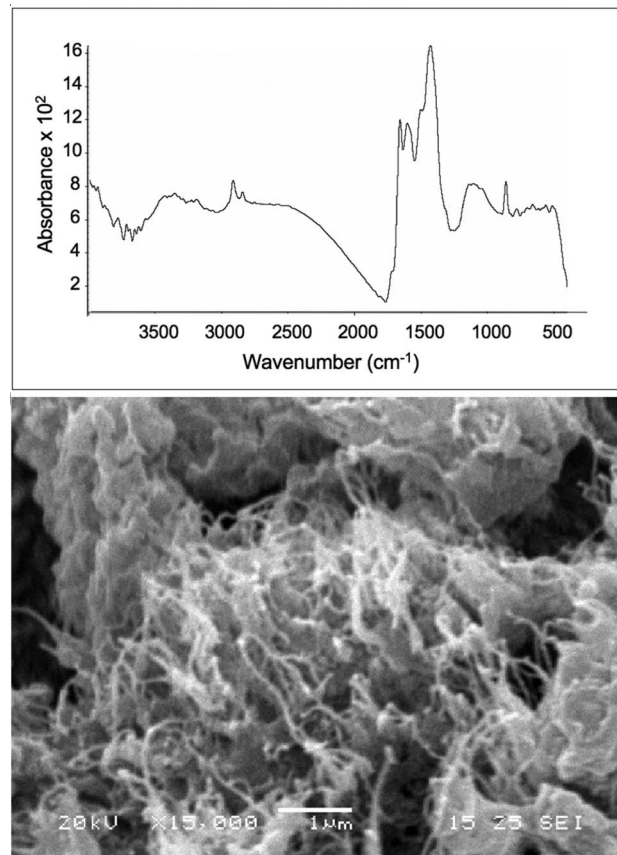


**Figure 4.** Poly(methyl  $\alpha$ -acetamidoacrylate)-grafted SWNT **8**. Top: FTIR spectrum. Bottom: SEM image. Magnification 15 000 $\times$ , scale bar 1  $\mu$ m.

reaction. Owing to the simplicity and smooth reaction conditions required, this “one-pot” procedure to functionalize SWNT should be practicable for a wide variety of electrophiles and vinyl monomers, as anticipated by the grafting of methyl  $\alpha$ -acetamidoacrylate.

**Acknowledgment.** We thank Gobierno Vasco (ETORTEK-BiomaGUNE IE-05/143 and ETORTEK NANOMATERIALES Program) for financial support. A Grant from Gobierno Vasco (Programa de Formación de Doctores en la Red Vasca de Ciencia, Tecnología e Innovación de los Departamentos de Industria, Comercio y Turismo y del Departamento de Educación, Universidades e Investigación”, “Fundación Centros Tecnológicos Iñaki Goenaga”) to A.G.-G. is acknowledged.

CM800625K

(20) Goodall, K.; Parsons, A. F. *Tetrahedron Lett.* **1995**, *36*, 3259–3260.